Research

Staufen 2 regulates mGluR long-term depression and Map1b mRNA distribution in hippocampal neurons

Geneviève Lebeau,[1,4] Linda C. Miller,[2,4] Maylis Tartas,[1] Robyn McAdam,[2] Isabel Laplante,[1] Frédérique Badeaux,[3] Luc DesGroseillers,[3] Wayne S. Sossin,[2,5] and Jean-Claude Lacaille[1,5]

[1]*Département de physiologie, GRSNC, Université de Montréal, Montréal, Québec H3C 3J7, Canada;* [2]*Department of Neurology and Neurosurgery, McGill University, Montreal, Quebec H3A 2B4, Canada;* [3]*Département de biochimie, GRSNC, Université de Montréal, Montréal, Québec H3C 3J7, Canada*

The two members of the Staufen family of RNA-binding proteins, Stau1 and Stau2, are present in distinct ribonucleoprotein complexes and associate with different mRNAs. Stau1 is required for protein synthesis–dependent long-term potentiation (L-LTP) in hippocampal pyramidal cells. However, the role of Stau2 in synaptic plasticity remains unexplored. We found that unlike Stau1, Stau2 is not required for L-LTP. In contrast, Stau2, but not Stau1, is necessary for DHPG-induced protein synthesis-dependent long-term depression (mGluR-LTD). While Stau2 is involved in early development of spines, its down-regulation does not alter spine morphology or spontaneous miniature synaptic activity in older cultures where LTD occurs. In addition, Stau2, but not Stau1, knockdown reduces the dendritic localization of Map1b mRNA, a specific transcript involved in mGluR-LTD. Moreover, mGluR stimulation with DHPG induces Map1b, but not Map2, mRNA dissociation from mRNA granules containing Stau2 and the ribosomal protein P0. This dissociation was not observed in cells in which Stau2 was depleted. Finally, Stau2 knockdown reduces basal Map1b protein expression in dendrites and prevents DHPG-induced increases in dendritic Map1b protein level. We suggest a role for Stau2 in the generation and regulation of Map1b mRNA containing granules that are required for mGluR-LTD.

[Supplemental material is available for this article.]

mRNA transport allows for production of proteins at a specific place and time (Holt and Bullock 2009). Sequences in the mRNA determine localization by providing binding sites for mRNA-binding proteins that mediate inclusion into specialized mRNA–protein transport complexes (Andreassi and Riccio 2009). These complexes (1) enable repression of the mRNA during transport, (2) provide association with motor proteins, and (3) confer specific mechanisms for translation activation of the mRNA (Sanchez-Carbente and DesGroseillers 2008). These RNA–protein transport complexes can be broadly separated into two types: (1) RNA granules containing ribosomes postulated to correspond to stalled polysomes and (2) RNA transport complexes lacking ribosomes and stalled at translation initiation (Sossin and DesGroseillers 2006).

Neurons use mRNA transport during development to regulate axon determination (Morita and Sobue 2009), growth cone turning (Lin and Holt 2007), neurite outgrowth (Hengst et al. 2009), and synapse maturation (Miniaci et al. 2008; Sebeo et al. 2009). After maturation, neurons use local translation both to concentrate proteins at specific sites and to respond to inputs in a local fashion by local changes in the proteome that regulate synaptic strength (Sutton and Schuman 2006; Bramham and Wells 2007; Sanchez-Carbente and DesGroseillers 2008).

[4]These authors contributed equally to this work.
[5]Corresponding authors.
E-mail jean-claude.lacaille@umontreal.ca; fax (514) 343-2111.
E-mail wayne.sossin@mcgill.ca
Article is online at http://www.learnmem.org/cgi/doi/10.1101/lm.2100611.

In particular, local translation of mRNAs is important for the late forms of long-term potentiation (L-LTP) and mGluR long-term depression (LTD) (Huber et al. 2000; Bradshaw et al. 2003). In mGluR-LTD, pre-localized mRNAs are translationally activated, and thus transcription is not required (Huber et al. 2000). The newly formed proteins mediate LTD by stimulating the endocytosis of AMPA receptors and allowing retention of these receptors in an internal pool (Bramham et al. 2008; Waung et al. 2008). Specifically, both Arc and Map1b are translationally up-regulated during mGluR-LTD and are known to be required for the maintenance of this form of plasticity (Davidkova and Carroll 2007; Waung et al. 2008). In L-LTP, translation of both preexisting mRNAs and mRNAs transported after de novo synthesis is important for the maintenance of L-LTP.

It would be interesting if particular RNA-binding proteins were involved in specific forms of plasticity, suggesting co-regulation of plasticity-related proteins. Recently, we showed that the RNA-binding protein Staufen 1 (Stau1) is required for L-LTP (Lebeau et al. 2008). In vertebrates, there are two members of the Staufen protein family, Stau1 and Staufen 2 (Stau2), that are constituents of distinct RNA granules in neurons (Duchaine et al. 2002). In this study, we compare the effects of removing Stau1 and Stau2 on L-LTP and mGluR-LTD. Strikingly, Stau1 down-regulation impairs only L-LTP, while Stau2 knockdown alters only mGluR-LTD, demonstrating specific roles for these two proteins in distinct forms of plasticity. Removal of Stau2 specifically decreases transport of a reporter with the Map1b 3′-UTR, while DHPG, an inducer of mGluR-LTD, dissociates Stau2 from Map1b

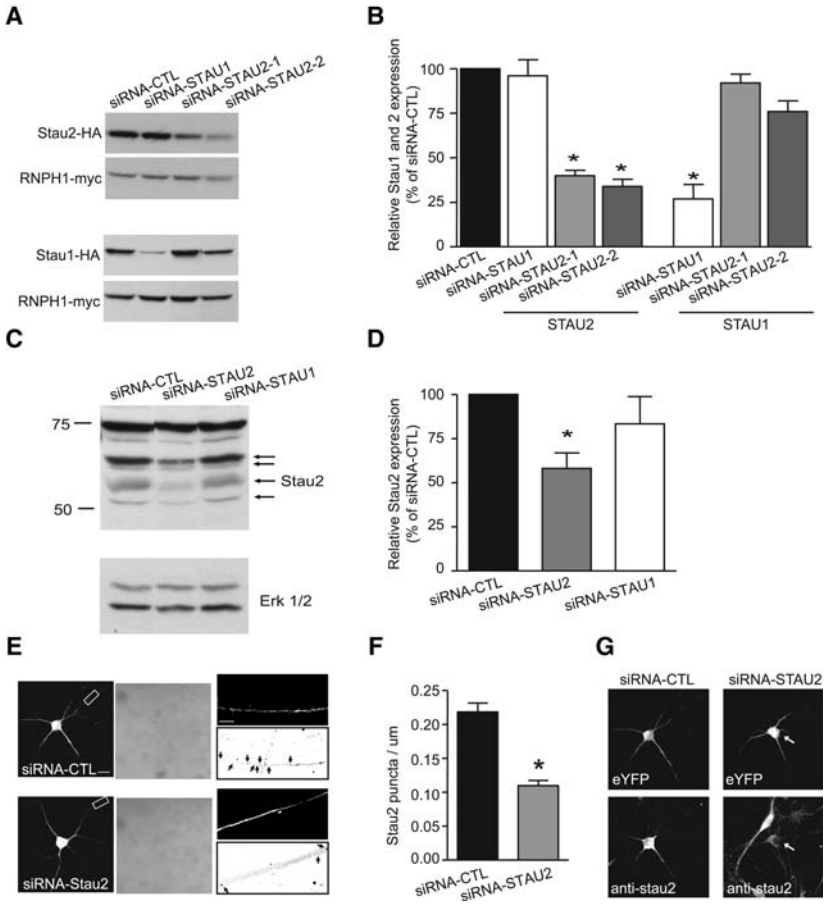

Figure 1. Knockdown of Stau2 by siRNA in HEK293 cells, hippocampal slice cultures, and primary hippocampal neurons. (*A*,*B*) Stau2 protein expression level was monitored by Western blotting in HEK293 cells. HEK293 cells were cotransfected with plasmids coding for hnRNPH1-myc and either mStau2-HA or mStau1-HA, as well as either siRNA-CTL, siRNA-STAU1, siRNA-STAU2-1, or siRNA-STAU2-2 (*A*). Expression of the proteins was analyzed using anti-HA and anti-myc antibodies and plotted as the percentage of expression of Stau1-HA or Stau2-HA compared to that of hnRNPH1-myc (*B*). Expression of Stau2-HA and Stau1-HA in cells with siRNA-CTL was set to 100%. Protein expression level (%) of Stau2, but not of Stau1, is significantly down-regulated in cells transfected with both siRNAs against Stau2. Protein expression level (%) of Stau1, but not of Stau2, is significantly down-regulated in cells transfected with siRNA-STAU1. (*C*,*D*) Stau2 protein expression level was monitored by Western blotting in older mature hippocampal slice cultures (21–24 d) biolistically transfected with siRNA-CTL, siRNA-STAU2-1, or siRNA-STAU1. Stau2-1 siRNA significantly decreases the amount of the four endogenous Stau2 isoforms (arrows point to 62, 59, 56, and 52 kDa, respectively; normalized to Erk level). (*E*–*G*) Representative neurons from primary cultures cotransfected with EYFP and siRNA-CTL or si-RNA-STAU2-1, and stained for endogenous Stau2. (*Left* panels) EYFP expressing neurons with the box indicating the area shown in the *right* panels. (*Center* panels) DIC images of the neurons. (*Right* panels) The *top* image is the EYFP-expressing dendrite; the *bottom* image is the endogenous Stau2. (Arrows) Stau2 puncta. (*F*) Quantification of the number of Stau2 puncta/μm >50 μm from the cell body ($n = 30$, siRNA-CTL; $n = 33$, siRNA-STAU2-1; three to four independent experiments). (*G*, *left* panels) siRNA-CTL transfected neurons. (*Right* panels) siRNA-STAU2-1 transfected neurons. (*Top* images) eYFP expression; (*bottom* images) endogenous Stau2. The arrows in *right* panels indicate an siRNA-STAU2-1-transfected cell beside an untransfected cell. $^*P < 0.05$, *t*-test. Error bars represent SEM; scale bars, 20 μm and 10 μm for *inset*.

3′-UTR puncta that colocalize with the ribosomal protein P0, suggesting an action on mRNA granules.

Results

Down-regulation of Stau2 by siRNA transfection

The efficacy and specificity of the siRNAs against Stau1 and Stau2 were tested by Western blot analysis in human embryonic kidney cells (HEK293) and in mature hippocampal slice cultures (21–24 d). First, HEK293 cells were cotransfected with plasmids coding for mStau1-HA or mStau2-HA and hnRNPH1-myc (used as control), as well as either a non-targeting siRNA (siRNA-CTL) or an siRNA directed against Stau1 or Stau2 (siRNA-STAU1, siRNA-STAU2-1, and siRNA-STAU2-2) (Fig. 1A,B). Western blot analysis with anti-HA and anti-myc antibodies indicated a significant reduction in the amounts of Stau2-HA relative to hnRNPH1-myc when cotransfected with siRNA-STAU2-1 (39.7% ± 3.2% of control; $n = 3$; $^*P < 0.05$; Student's *t*-test) and siRNA-STAU2-2 (34.3% ± 3.9% of control; $n = 3$; $^*P < 0.05$; Student's *t*-test), compared to siRNA-CTL (Fig. 1A,B). When plasmid coding for Stau1-HA instead of Stau2-HA was transfected in HEK293 cells, no significant decrease in the expression of Stau1 protein was observed in the presence of either siRNA-STAU2 compared to siRNA-CTL (siRNA-STAU2-1: 92.0% ± 5.1% of control; siRNA-STAU2-2: 76.3% ± 6.2% of control; $n = 3$; $P > 0.05$; Student's *t*-test) (Fig. 1A,B). These results indicate that transfection of both siRNAs against Stau2 is efficient in down-regulating the expression of Stau2 and the down-regulation is specific, leaving Stau1 levels intact. We observed the same efficacy and specificity of Stau1 siRNA on Stau1-HA and Stau2-HA expression levels (Stau1-HA: 26.7% ± 7.5% of control; $^*P < 0.05$; Stau2-HA: 96.3% ± 8.7% of control; $n = 3$; $P > 0.05$; Student's *t*-test) (Fig. 1A,B).

Next, we tested the efficacy of siRNA-STAU2-1 transfection to down-regulate endogenous Stau2. Biolistic siRNA delivery was performed in 14 DIV slice cultures with either a nontargeting siRNA (siRNA-CTL), or siRNA directed against Stau1 (siRNA-STAU1) or Stau2 (siRNA-STAU2-1). While biolistic DNA plasmid transfection in organotypic slice cultures leads to only a small percentage of transfected neurons (1%–2%) (Wellmann et al. 1999; Boda et al. 2004; Govek et al. 2004), we have found that delivery of siRNAs is much more efficient (Lebeau et al. 2008). Indeed, using a fluorescently labeled siRNA, one can detect high levels of siRNA in most of the superficial principal neurons in slices where the electrophysiological recordings are performed (Lebeau et al. 2008). The higher transfection efficiency may be due to the requirement for plasmid DNAs to penetrate not only the plasma membrane but also the nuclear membrane for effectiveness, while siRNA is effective in the cytoplasm. Efficient knockdown using siRNA in organotypic slice cultures has also been seen in other studies (Murphy et al. 2008; Dominguez et al. 2009). Two days post-transfection, slices were homogenized and analyzed by Western blotting using anti-Stau2 antibody

(Fig. 1C). Slices transfected with siRNA-STAU2-1 revealed a significant reduction in endogenous Stau2 expression level compared to slices transfected with siRNA-CTL (58.1% ± 8.8% of control; $n = 6$, two independent experiments; $^*P < 0.05$) (Fig. 1D). Since the entire slices were taken for Western blot experiments, while only the neurons at the superficial level receive siRNA, the results from this analysis underestimate the knockdown in the neurons recorded in field recording experiments (Lebeau et al. 2008). Stau2 expression levels were not significantly altered in slices transfected with siRNA-STAU1 (83.4% ± 15.5% of control). These results indicate that transfection of siRNA-STAU2-1 is efficient and specific in down-regulating the expression of Stau2 protein. Efficacy and selective knockdown of Stau1 endogenous protein levels by siRNA-STAU1 were tested previously (Lebeau et al. 2008), and a 32% decrease of protein level expression was observed, similar to the 42% decrease seen for Stau2. Next, we verified Stau2 knockdown efficacy in individual cells by transfecting primary hippocampal cultures with siRNA-CTL or siRNA-STAU2-1 on 13 DIV and fixing the cells on 15 DIV. The neurons were immunostained for endogenous Stau2, confirming that the knockdown was effective in dendrites and soma (Fig. 1E–G).

Stau2 knockdown does not block L-LTP

Local translation of mRNAs in dendrites is required for synaptic plasticity (Kiebler and DesGroseillers 2000; Steward and Schuman 2001). The RNA-binding proteins Stau1 and Stau2, known to be involved in mRNA trafficking to neuronal dendrites (Kanai et al. 2004; Kim and Kim 2006) and translational regulation (Dugre-Brisson et al. 2005), are good candidates for regulating synaptic plasticity. Indeed, we recently showed that Stau1 is involved in the late form of LTP (L-LTP) (Lebeau et al. 2008), a synaptic plasticity process that requires both transcription and translation (Krug et al. 1984; Frey et al. 1988; Otani et al. 1989; Nguyen et al. 1994). However, the role of Stau2 in synaptic plasticity remains undetermined. Therefore, we first studied the consequence of Stau2 knockdown on forskolin (FSK)-induced L-LTP of CA1 fEPSPs in young mature hippocampal slice cultures (11–14 d) and compared it to that reported for Stau1. This L-LTP is NMDAR-dependent and is blocked by actinomycin D (Lebeau et al. 2008). Slice cultures were biolistically cotransfected with plasmid coding for EYFP and siRNA-CTL, siRNA-STAU1, or siRNA-STAU2-1. In slices transfected with siRNA-CTL, application of FSK induced L-LTP of fEPSPs lasting at least 3.5 h (164.9% ± 13.3% of control; $n = 5$; $^*P < 0.05$) (Fig. 2A,B). As expected, FSK-induced L-LTP was blocked in slices transfected with siRNA-STAU1 (105.6% ± 7.9% of control; $n = 7$; $P > 0.05$) (Fig. 2A,B). In contrast, FSK-induced L-LTP was not impaired after Stau2 knockdown (175.0% ± 12.8% of control; $n = 5$; $^*P < 0.05$) (Fig. 2A,B). The depression of fEPSP responses in the first 60 min after LTP induction is due to FSK-induced spontaneous activity interfering with fEPSPs measures (Otmakhov et al. 2004; Kopec et al. 2006). Similar forskolin-induced spontaneous synaptic activity was observed in all three groups. Moreover, basal synaptic transmission was unchanged after knockdown of Stau1 or Stau2, as shown by input–output function ($n = 6$ to 8; $P > 0.05$) (Fig. 2C) and paired-pulse facilitation ratio (at intervals of 50 to 150 msec) of fEPSPs ($n = 4$ to 8; $P > 0.05$) (Fig. 2D). These results indicate that Stau2 is not required for FSK-induced L-LTP, and thus Stau1 and Stau2 do not share a similar role in this form of synaptic plasticity.

mGluR-LTD is impaired by Stau2 knockdown

Next, we determined whether Stau2 is involved in translation-dependent mGluR1/5-mediated long-term depression (mGluR-LTD) in slice cultures. Activation of mGluR1/5 by the selective agonist DHPG produces LTD, which requires local translation of dendritic mRNAs in mature neurons, but not earlier in development (Fitzjohn et al. 1999; Huber et al. 2000; Nosyreva and Huber 2005). First, we established that mGluR1/5-mediated LTD is protein synthesis-dependent in our slice culture model. As expected, application of DHPG in older mature slice cultures (21–24 d) induced LTD of fEPSPs in siRNA-CTL transfected slices (63.1% ± 2.9% of control; $n = 5$; $^*P < 0.05$) (Fig. 3A,D), which was dependent on protein synthesis as it was completely blocked by application of rapamycin (98.1% ± 9.3% of control; $n = 7$; $P > 0.05$) (Fig. 3A,D).

Next, we examined the importance of Stau2 expression for mGluR-LTD. We showed previously that Stau1 knockdown does not affect translation-independent DHPG-induced LTD in young mature hippocampal slice cultures (11–14 d) (Lebeau et al. 2008). Thus, we tested translation-dependent mGluR-LTD in older mature slice cultures (21–24 d) transfected with siRNA-STAU1, siRNA-STAU2-1, siRNA-STAU2-2, or siRNA-CTL. Stau1 down-regulation had no effect on mGluR-LTD since application of DHPG induced a similar fEPSP depression in slices transfected with siRNA-STAU1 (74.0% ± 13.7% of control; $n = 7$; $^*P < 0.05$)

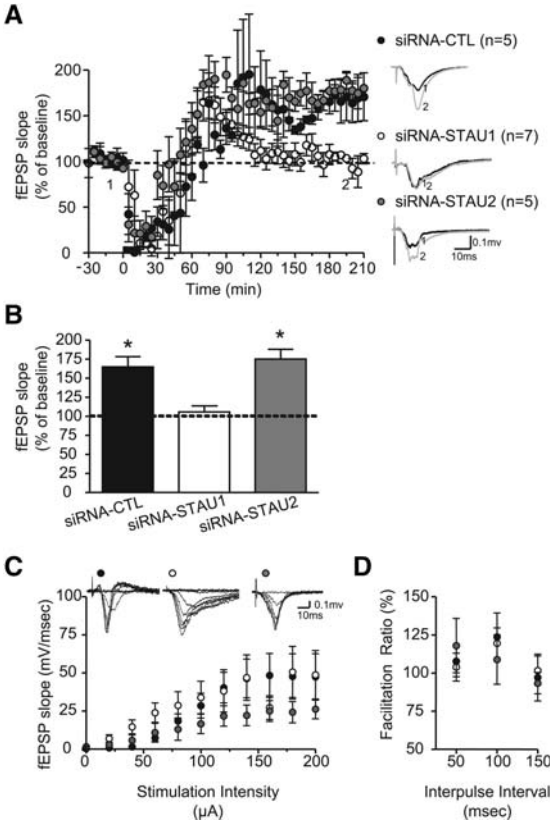

Figure 2. Stau2 siRNA does not prevent FSK-induced L-LTP. (*A*) Potentiation of fEPSP slope induced by FSK application (50 μM, 15 min) in mature cultured slices transfected with siRNA-CTL, siRNA-STAU1, and siRNA-STAU2-1. Corresponding field potentials before (black line) and after (gray line) FSK application are shown at *right*. (*B*) Summary bar graph showing changes in fEPSPs slope 200 min post-FSK application. Significant L-LTP was present in slices transfected with siRNA-CTL and siRNA-STAU2-1 but absent in slices transfected with siRNA-STAU1, indicating that only Stau1 knockdown prevents L-LTP. $^*P < 0.05$, *t*-test. Error bars represent SEM. (*C*,*D*) Stau1 and Stau2 siRNA transfection did not affect basal synaptic transmission ([*C*] input–output function; [*D*] paired-pulse facilitation ratio).

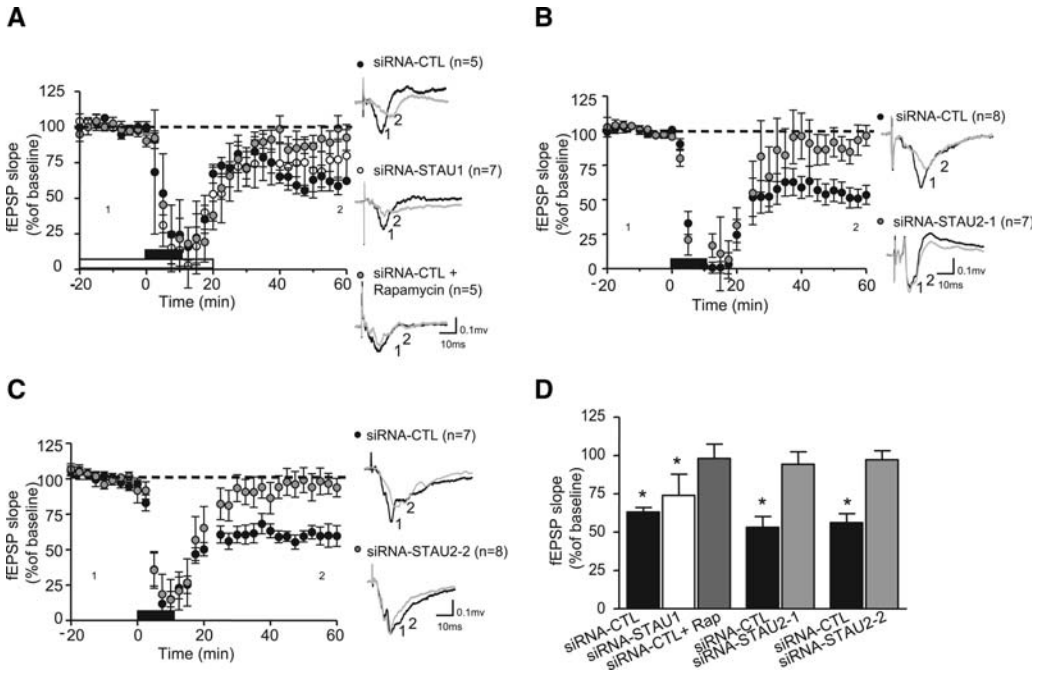

Figure 3. Stau2 siRNA impairs mGluR-induced protein synthesis-dependent LTD. (*A*) Long-term depression of fEPSP slope induced by DHPG application (100 μM, 10 min) in older mature slice cultures transfected with siRNA-CTL and siRNA-STAU1. LTD is blocked by the protein synthesis inhibitor rapamycin (200 nM, 20 min before and after LTD induction; siRNA-CTL transfection). Corresponding field potentials before (black line) and after (gray line) DHPG application are shown at *right*. (*B*,*C*) DHPG-induced LTD is blocked by two different Stau2 siRNAs, siRNA-STAU2-1 (*B*) and siRNA-STAU2-2 (*C*). Corresponding field potentials before (black line) and after (gray line) DHPG application are shown at *right*. (*D*) Summary bar graph showing changes in fEPSPs slope 60 min post-DHPG application. Significant LTD was present in slices transfected with siRNA-CTL and siRNA-STAU1, but was blocked by rapamycin, indicating that mGluR-induced LTD is protein synthesis-dependent in older mature slice cultures. Stau2 siRNA transfection prevented DHPG-induced LTD, indicating that only Stau2 knockdown impairs mGluR-LTD. $^*P < 0.05$, *t*-test. Error bars represent SEM.

(Fig. 3A,D). These results suggest that Stau1 is not implicated in protein synthesis-dependent mGluR-LTD. In contrast, knockdown of Stau2 by two different siRNAs prevented mGluR-LTD (siRNA-CTL: 53.2% ± 6.9% of control; $n = 8$; $^*P < 0.05$; siRNA-STAU2-1: 94.2% ± 8.1% of control; $n = 7$; $P > 0.05$; siRNA-STAU2-2: 97.1% ± 5.9% of control; $n = 8$; $P > 0.05$) (Fig. 3B–D). These results indicate that, in contrast to Stau1, Stau2 is necessary for mGluR-LTD. Taken together, our results provide strong evidence for subtype-specific roles of Stau1 and Stau2 in translation-dependent forms of long-term plasticity, with Stau1 critically implicated in FSK-induced L-LTP and Stau2 essentially involved in mGluR1/5-mediated LTD.

Stau2 down-regulation alters spine morphology in young but not older slice cultures

It was previously shown that Stau2 down-regulation alters spine morphogenesis (Goetze et al. 2006). In order to understand the role of Stau2 in mGluR-LTD at a cellular level, we next examined if Stau2 knockdown induces some changes in dendritic spine density and morphology in young (11–14 d) and older (21–24 d) mature slice cultures where protein synthesis-dependent mGluR-LTD occurs. Therefore, hippocampal slices were transfected with plasmids coding for EYFP and either siRNA-STAU2-1 or siRNA-CTL. Confocal imaging of EYFP-labeled cells showed no apparent alteration in the general dendritic arborization in any group (Fig. 4A). The overall spine density was unchanged among cells of young (11–14 d) versus older (21–24 d) groups and also was unaltered after Stau2 knockdown in either group, indicating, first, no notable increase in spine number in older mature slices, and, second, no loss of spines after Stau2 knockdown (Fig. 4B). To further characterize changes in spine morphology, we studied the distribution of different classes of protrusions categorized on length, shape, and spine head occurrence (McKinney 2005; Lebeau et al. 2008). In accordance with results obtained after Stau2 knockdown in neuronal cultures (Goetze et al. 2006), increases in spine length and incidence of elongated type of spines were observed in siRNA-STAU2-1-transfected cells of young (11–14 d) mature slices. The cumulative distribution of spine length was different, the mean spine length was increased (1.18 ± 0.03 μm for siRNA-STAU2-1 vs. 1.09 ± 0.02 μm for siRNA-CTL; $^*P < 0.05$) (Fig. 4C), and the proportion of elongated spines was augmented (46.4% ± 2.1% of total spine number for siRNA-STAU2-1 compared to 39.4% ± 2.4% for siRNA-CTL; $^*P < 0.05$) (Fig. 4D). In contrast, no changes in dendritic spine length and proportion of elongated spines were seen after Stau2 knockdown in older (21–24 d) mature slice cultures (Fig. 4C,D). Thus, Stau2 appears to have a role early in the development of dendritic spine morphogenesis. However, this function is no longer present in older (21–24 d) mature slice cultures at stages when Stau2 plays an essential role in mGluR-LTD, indicating a dissociation of its role in spine alterations and mGluR-LTD.

Miniature synaptic activity is not affected by Stau2 knockdown

We next tested whether Stau2 down-regulation was associated with functional changes at unitary excitatory synapses in older mature slices (21–24 d). We recorded miniature EPSCs (mEPSCs) in EYFP-transfected CA1 pyramidal cells voltage-clamped at

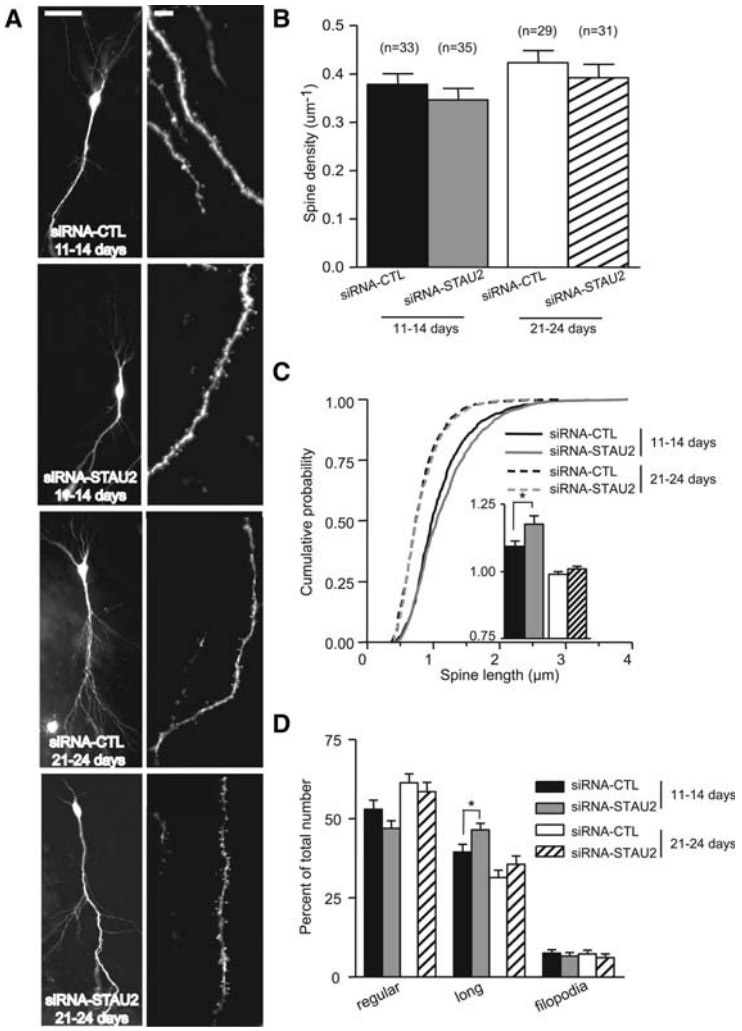

Figure 4. Stau2 siRNA does not affect pyramidal cell spine morphology in older mature slice cultures. (*A*) Confocal images of representative CA1 pyramidal cells (*left*) and apical dendrites (*right*) after transfection with siRNA-CTL and siRNA-STAU2-1 in young (11–14 d) and older (21–24 d) mature slice cultures. (*B*) Spine density was unchanged by Stau2 siRNA transfection in either age group. (*C*) Cumulative plots of the distribution of spine length for each group, with summary bar graph of spine length in the *inset*, showing increased spine length after Stau2 siRNA transfection only in young mature slice cultures. (*D*) Summary bar graph of the number of regular, elongated, and filopodium types of spines in each group, showing an increase in elongated spines after Stau2 siRNA transfection only in young mature slice cultures. Scale bars, 25 μm, 5 μm. $^{*}P < 0.05$, *t*-test. Error bars represent SEM.

−60 mV and examined the effect of siRNAs on amplitude and frequency of synaptic activity (Fig. 5A). Stau2 siRNA transfection did not affect miniature synaptic activity. The cumulative distributions of mEPSC amplitude and frequency were unchanged in neurons transfected with siRNA-STAU2-1 relative to neurons transfected with siRNA-CTL ($n = 6$ each, six slices, four independent experiments, $P > 0.05$; Kolmogorov-Smirnov test) (Fig. 5B,C). The lack of effect on miniature synaptic activity in mature slices suggests that Stau2 down-regulation does not affect basal transmission at individual excitatory synapses, which is consistent with the unaffected spine morphology.

Stau2 knockdown reduces endogenous Maplb protein in dendrites

Staufens are RNA-binding proteins; thus we examined next whether the block of mGluR-LTD was associated with changes in translation of mRNAs known to be involved in this plasticity. Map1b protein level increases during DHPG-induced LTD, and this increase is required for endocytosis of AMPARs (Hou et al. 2006; Davidkova and Carroll 2007). We thus investigated whether Stau2 knockdown regulated endogenous Map1b levels using immunocytochemistry in cultured hippocampal neurons at 48 h post-transfection with siRNA-CTL or siRNA-STAU2-1. Map1b was extensively expressed in dendrites of hippocampal neurons transfected with siRNA-CTL, and 20 μM DHPG treatment significantly increased dendritic levels of Map1b protein (120.9% ± 4.04% of vehicle-treated siRNA-CTL; $^{*}P < 0.05$; ANOVA) (Fig. 6A,B). Knockdown of Stau2 significantly decreased the level of endogenous Map1b protein (55.80% ± 4.68% of vehicle-treated siRNA-CTL; $^{**}P < 0.01$; ANOVA) and prevented the DHPG-induced increase in Map1b protein levels (58.15% ± 6.30% of vehicle-treated siRNA-CTL; $^{**}P < 0.01$; ANOVA) (Fig. 6A,B). Our results reveal a functional link between Stau2 and expression of endogenous Map1b protein in dendrites. Moreover, these observations are consistent with a model in which knockdown of Stau2 blocks mGluR-LTD by preventing translation of mGluR-LTD-related mRNAs.

Stau2 knockdown reduces the amount of Maplb mRNA in dendrites

We then tested at the molecular level if Stau2 down-regulation alters the transport/distribution of Map1b mRNA. We made use of the MS2 reporter system in which a chimeric mRNA that contains multiple MS2-binding sites (MS2bs) in its 3′-UTR is detected by the binding of a fluorescently tagged MS2 protein (Rook et al. 2000). In this study, we used the luciferase ORF on which was fused 24 copies of the MS2-binding site and either the Map1b, the α-CaMKII, or the MAP2 3′-UTR. Map1b, α-CaMKII, and MAP2 3′-UTR contain dendritic targeting elements, and α-CaMKII is an mRNA translated during L-LTP and is a known target of Stau1 (Kanai et al. 2004). When these mRNA reporters were cotransfected into hippocampal neurons with NLS-MS2-mCherry, distinct puncta were seen in dendrites >50 μm from the cell body, indicating that the mRNAs are being transported (Supplemental Fig. S1). Very few puncta were seen in the absence of a cotransfected MS2bs-containing mRNA (Supplemental Fig. S1). Primary hippocampal cultures (13 DIV) were cotransfected with a plasmid coding for EYFP to visualize the neuron and with siRNA-CTL, siRNA-STAU1 or siRNA-STAU2-1, Luc-24xMS2bs-Map1b 3′-UTR or Luc-24xMS2bs-CaMKII 3′-UTR, and NLS-MS2-mCherry. Cells were fixed 48 h post-transfection. The number of mRNA: MS2-mCherry puncta was determined by Image J software (with the analyze particles task) and counted in 30–50-μm

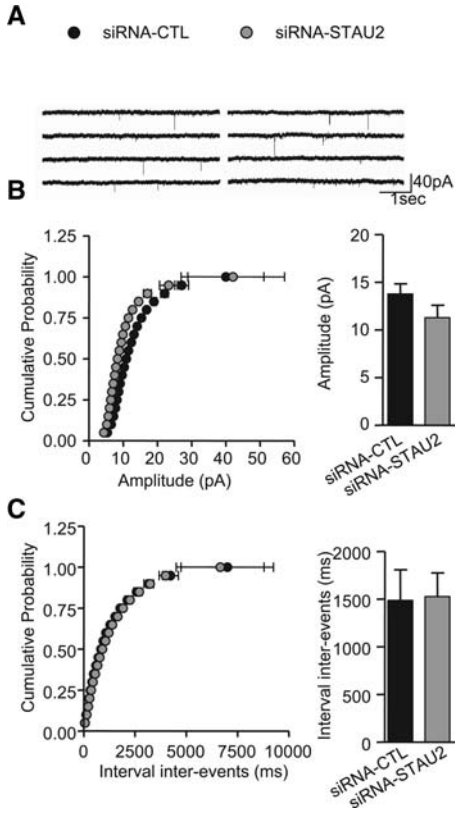

Figure 5. Spontaneous miniature synaptic activity is not affected by Stau2 knockdown. Stau2 siRNA transfection does not impair frequency and amplitude of mEPSCs. (*A*) Representative traces from pyramidal neurons transfected with siRNA-CTL (*left*) or siRNA-STAU2-1 (*right*) in older (21–24 d) mature slice cultures. (*B*,*C*) Summary plots of cumulative distribution and summary bar graph of mEPSC amplitude (pA) (*B*) and inter-mEPSC intervals (msec) (*C*) for the corresponding groups ($n = 6$ cells in each group) showing no changes in amplitude and frequency of mEPSCs in neurons transfected with siRNA-STAU2-1. Error bars represent SEM.

segments of dendrites at least 50 μm from the cell body to determine the effect of the knockdown on the transport of the reporter mRNAs. There was a significant decrease in the number of Luc-24xMS2bs-Map1b mRNA puncta in cells transfected with siRNA-STAU2-1 compared to siRNA-CTL (Fig. 7E,F) (0.14 ± 0.01 puncta/μm compared to 0.22 ± 0.02 puncta/μm; $^{*}P < 0.05$; $n =$ 41 and 34 dendritic segments, respectively; three to four independent experiments; ANOVA), while there was no decrease in the number of control Luc-24xMS2bs puncta (Fig. 7A,B) or Luc-24xMS2bs-CaMKII mRNA puncta (Fig. 7C,D) (0.21 ± 0.02 puncta/μm compared to 0.23 ± 0.02 puncta/μm). In contrast, knockdown of Stau1 specifically decreased the transport of Luc-24xMS2bs-CaMKII mRNA (0.18 ± 0.01 puncta/μm compared to 0.23 ± 0.01 puncta/μm in control, $\#P < 0.05$ one-tailed test, ANOVA) and did not affect the transport of Luc-24xMS2bs-Map1b mRNA (0.25 ± 0.02 puncta/μm compared to 0.22 ± 0.02 puncta/μm) or control Luc-24xMS2bs puncta (Fig. 7A–F). This specificity of Stau1 and Stau2 interactions with L-LTP- and mGluR-LTD-related mRNAs, respectively, is consistent with the effect of their respective knockdown on synaptic plasticity in slice cultures. The lack of an effect of Stau2 knockdown on transported levels of the CAMKII and Map2 3′-UTR reporter mRNAs suggest that Stau2 knockdown does not prevent transport of all mRNAs.

Luc-24xMS2bs-Map1b 3′-UTR mRNA is found in both RNA granules and RNA particles

We next wanted to determine the type of structure (RNA granules containing ribosomes or RNA transport structures lacking ribosomes) in which Luc-24xMS2bs-Map1b mRNA was found. Primary hippocampal neurons were cotransfected with plasmids coding for Stau2-GFP, NLS-MS2-mCherry, and Luc-24xMS2bs-Map1b at 13 DIV. Cells were also immunostained with antibodies for the ribosomal marker P0 to follow the association of the mRNA constructs with ribosomes and, thus, distinguish between RNA granules and RNA transport particles (Sossin and Desgroseillers 2006). This experiment revealed that, of the total Luc-24xMS2bs-Map1b mRNA puncta, $37.4\% \pm 4.5\%$ contained Stau2-GFP (Fig. 8C), while $21.6\% \pm 3.9\%$ were P0 immunopositive (Fig. 9A). Moreover, $12.2\% \pm 2.2\%$ of the Luc-24xMS2bs-Map1b mRNA puncta colocalized with both Stau2-GFP and P0 (Supplemental Fig. S2). Therefore, about one-third of the Stau2-positive Luc-24xMS2bs-Map1b mRNA puncta have the characteristics of RNA granules (positive for P0), whereas more than half of Luc-24xMS2bs-Map1b RNA granules (positive for P0) contained

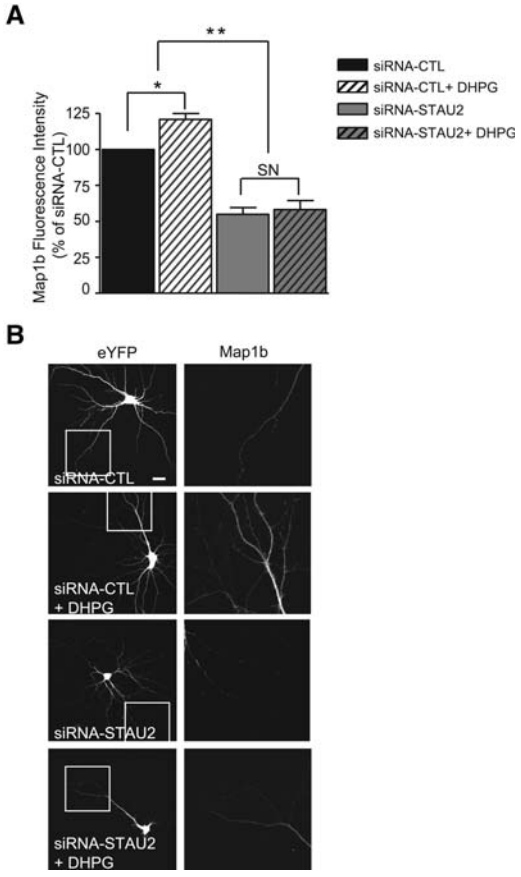

Figure 6. Stau2 knockdown decreases endogenous Map1b protein level and prevents DHPG-induced increases of Map1b in dendrites. (*A*, *B*) Immunocytochemistry for endogenous Map1b protein in neurons transfected with EYFP and siRNA-CTL or siRNA-STAU2-1. (*A*) Summary bar graph of endogenous Map1b protein level in dendrites (50 to 100 μm from the cell body), with and without DHPG treatment (20 μM). (*B*) Confocal images of representative neurons transfected with siRNA-CTL and siRNA-STAU2-1, with or without DHPG treatment (eYFP, *left*; Map1b, *right*). The boxed area in the *left* panels indicates region shown at higher magnification in *right* panels. $^{*}P < 0.05$, $^{**}P <$ 0.01, ANOVA. Error bars represent SEM. Scale bar, 20 μm.

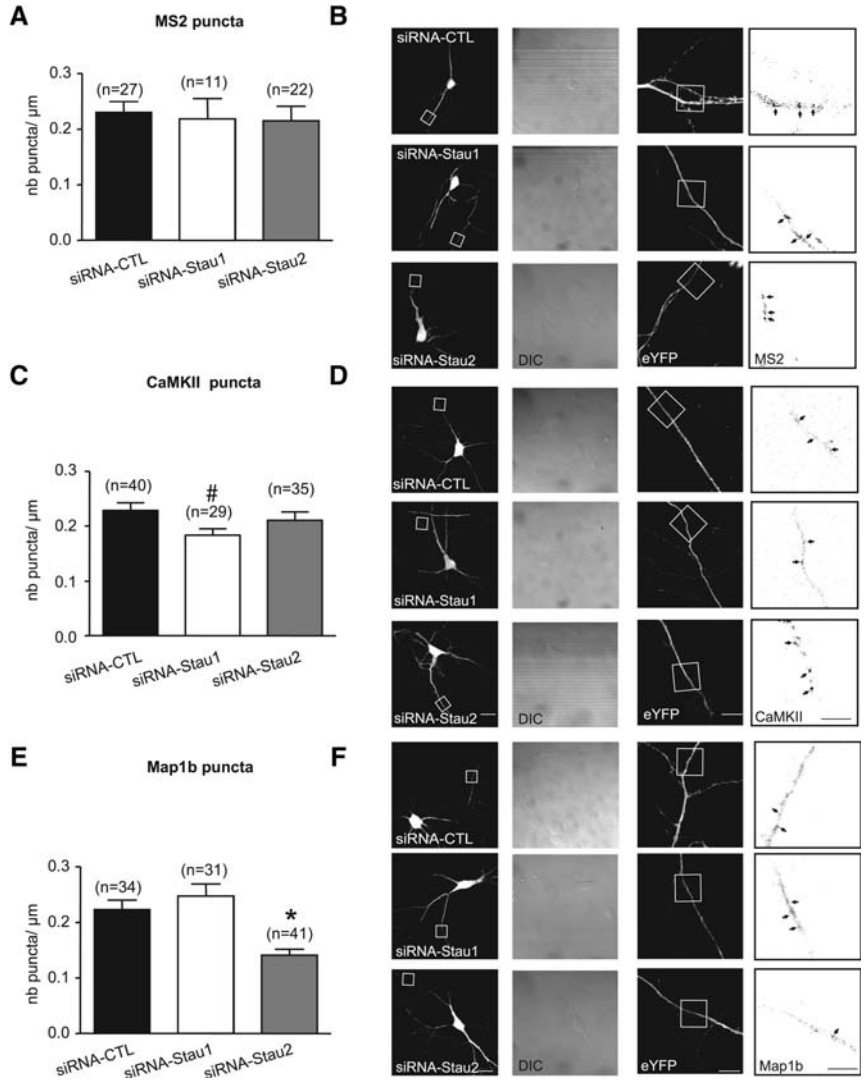

Figure 7. Stau2 knockdown reduces transport of Luc-24xMS2bs-Map1b 3′-UTR mRNA. (*A*,*C*,*E*) Summary bar graphs of the number of NLS-MS2-mCherry puncta/µm >50 µm from the cell body in cells transfected with EYFP and NLS-MS2-mCherry, siRNAs (siRNA-CTL, siRNA-STAU1, or siRNA-STAU2-1), and mRNA reporters (Luc-24xMS2bs [*A*], Luc-24xMS2bs-CaMKII 3′-UTR [*C*], or Luc-24xMS2bs-Map1b 3′-UTR [*E*]). siRNA-STAU1 significantly decreases Luc-24xMS2bs-CaMKII 3′UTR mRNA (*C*), and siRNA-STAU2-1 significantly reduces Luc-24xMS2bs-Map1b 3′-UTR mRNA (*E*). (*B*,*D*,*F*) Confocal images of representative neurons transfected with siRNA-CTL (*top* panels), siRNA-STAU1 (*middle* panels), or siRNA-STAU2-1 (*bottom* panels), EYFP (cell [*left* panels], dendrite boxed area [*center right* panels]), and NLS-MS2-mCherry (*right* panels). DIC images are in the *center left* panels. Arrows point to mCherry puncta marking Luc-24xMS2bs mRNA (*B*), Luc-24xMS2bs-CaMKII 3′-UTR mRNA (*D*), or Luc-24xMS2bs-Map1b 3′-UTR mRNA (*F*). n = number of segments from three to four experiments. $^*P < 0.05$, ANOVA; $\#P < 0.05$, ANOVA one-tailed test. Error bars represent SEM. Scale bars, 20 µm and 10 µm.

Stau2-GFP. These results suggest that Map1b mRNA can be found in both RNA granules as well as RNA particles, and that a large percentage of the Map1b mRNA-containing granules are associated with Stau2.

Stau2 and P0 dissociate from Luc-24xMS2bs-Map1b 3′-UTR mRNA upon DHPG stimulation

Local de novo synthesis of Map1b protein is required for mGluR-LTD. Translational activation may involve dissociation of an mRNA–protein complex (Krichevsky and Kosik 2001; Huttelmaier et al. 2005). We thus asked if we could detect changes in the composition of Luc-24xMS2bs-Map1b 3′-UTR puncta after application of the mGluR-LTD induction protocol. Primary hippocampal neurons were cotransfected with plasmids coding for Stau2-GFP, NLS-MS2-mCherry, and either Luc-24xMS2bs-Map1b or Luc-24xMS2bs-Map2 3′-UTR at 13 DIV. Forty-eight hours post-transfection, cells were treated with 20 µM DHPG or vehicle, and fixed 10 min later. First, the number of puncta in dendritic areas >50 µm from the cell body was analyzed for each transfection condition. No differences were found in the total number of puncta before and after DHPG treatment (Supplemental Fig. S3), suggesting that DHPG treatment did not change overall expression and/or transport of these mRNA–protein transport complexes.

We next determined the percentage of colocalization of Stau2 and mRNAs for each condition. Interestingly, colocalization of Stau2 with Luc-24xMS2bs-Map1b mRNA was decreased after DHPG treatment (from 32.96% ± 3.84% to 21.92% ± 3% of total Stau2 puncta [Fig. 8A,B]; from 37.43% ± 4.5% to 24.32% ± 3.66% of total Map1b puncta [Fig. 8C,D]; $^*P < 0.05$; $n = 25–31$ dendritic segments; four independent experiments). In contrast, there was no change in the colocalization of Stau2 with Luc-24xMS2bs-Map2 mRNA after DHPG treatment (35.07% ± 3.31% and 33.91% ± 3.59% of total Stau2 puncta; 34.58% ± 3.5% and 35.21% ± 3.4% of total Map2 puncta) (Fig. 8A–D). Thus it appears that there is a subset of Stau2 granules that responds to DHPG treatment, and these contain Map1b mRNA, and vice versa.

Similarly, we observed a decrease in the colocalization of Luc-24xMS2bs-Map1b mRNA with P0 after DHPG treatment (from 21.61% ± 3.93% to 10.93% ± 2.91% of total Map1b puncta; $^*P < 0.05$; $n = 22$ and 23 segments; four different experiments) (Fig. 9A,B). Interestingly, the decrease in the colocalization of Luc-24xMS2bs-Map1b mRNA and P0 after DHPG treatment was abolished when Stau2 was knocked down with siRNA-STAU2-1. In these conditions, the colocalization of Luc-24xMS2bs-Map1b mRNA with P0 did not change after DHPG (28.83% ± 4.66% and 29.31% ± 6.16% of total Map1b puncta; $P > 0.05$; $n = 19$ and 20 segments; four different experiments) (Fig. 9A,B), suggesting that Map1b mRNA and P0 dissociation induced by mGluR activation is dependent on Stau2 and that Map1b mRNA not colocalized with Stau2 is not regulated by activation of mGluR during LTD. As control, Luc-24xMS2bs-Map2 mRNA colocalization with P0 was not significantly changed after DHPG treatment (Fig. 9). Altogether, these experiments indicate that mRNA complexes containing Staufen, P0, and Luc-24xMS2bs-Map1b mRNA are dissociated in response to mGluR activation, suggesting a

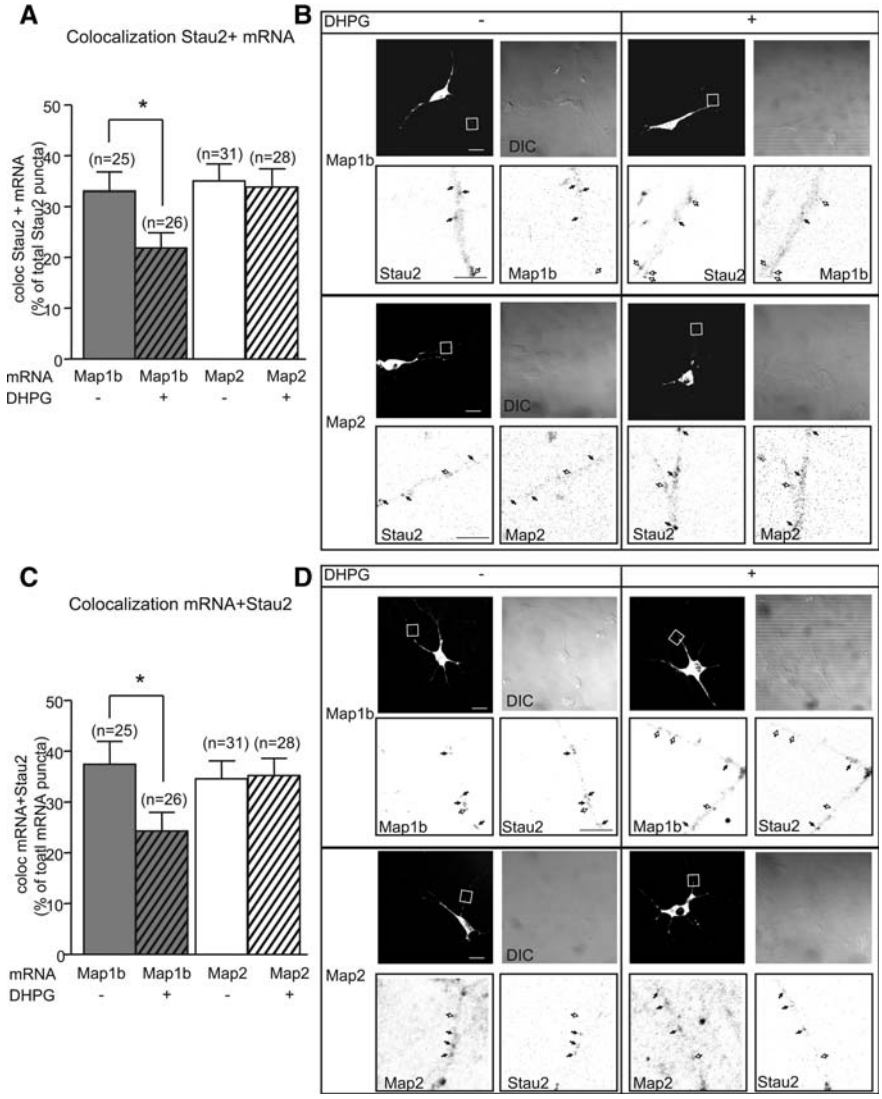

Figure 8. Luc-24xMS2bs-Map1b 3′-UTR mRNA dissociates from Stau2 upon application of DHPG. (*A, B*) Colocalization of Stau2-GFP with NLS-MS2-mCherry-labeled mRNA puncta in relation to Stau2 puncta in dendrites (>50 μm from the cell body), with and without DHPG treatment. (*A*) Summary bar graph of colocalization of Stau2-GFP and NLS-MS2-mCherry-labeled mRNA puncta as percentage of total Stau2-GFP puncta. (*B*) Confocal images of representative neurons transfected with Stau2-GFP (*left* images) and Luc-24xMS2bs-Map1b 3′-UTR or Luc-24xMS2bs-Map2 3′-UTR (*bottom right* images). DIC images are in the *top right*. The boxed area in the *top left* image indicates region shown in *bottom* images. Filled arrows indicate colocalized puncta, and open arrows indicate Stau2-GFP puncta alone. (*C,D*) Colocalization of NLS-MS2-mCherry-labeled mRNA puncta with Stau2-GFP in relation to mRNA presence. (C) Summary bar graph of colocalization of Stau2-GFP and NLS-MS2-mCherry-labeled mRNA puncta as percentage of total mRNA puncta. (*D*) Confocal images of representative neurons transfected with Stau2-GFP (*left* images) and Luc-24xMS2bs-Map1b 3′-UTR or Luc-24xMS2bs-Map2 3′-UTR (*bottom left* images). DIC images are in the *top right*. The boxed area in the *top left* image indicates region shown in *bottom* images. Filled arrows indicate colocalized puncta, and open arrows indicate mRNA puncta alone. Colocalization of Stau2-GFP and Luc-24xMS2bs-Map1b mRNA is decreased after DHPG treatment. n = number of segments from four experiments. $^*P < 0.05$, *t*-test. Error bars represent SEM. Scale bars, 20 μm and 10 μm.

Stau2-dependent regulation of Map1b mRNA-containing granules during mGluR-LTD induction.

Discussion

In neurons, localization of mRNAs at the synapse followed by their regulated translation is a mechanism for synaptic plasticity and thus learning and memory (Klann and Dever 2004). Our study provides evidence for a specific role for Stau2 protein in a particular form of plasticity, mGluR1/5-mediated LTD through regulation of mRNAs required for mGluR-LTD such as Map1b (Supplemental Fig. S4). Specifically, knockdown of Stau2 blocks this form of LTD, decreases both endogenous Map1b protein expression and the level of a reporter with the MAP1b 3′-UTR that is transported to dendrites, and prevents mGluR1/5-induced dissociation of the Map1b 3′-UTR reporter from P0-containing mRNA granules.

Specificity of RNA-transport complexes

An important issue in the role of translation in synaptic plasticity is whether different forms of plasticity induce translation of distinct proteins, or whether the translational regulation is general for all forms of stimulation and the type of plasticity is determined by individual synaptic modification. The phenomenon of cross-tagging suggests that both L-LTP and protein-synthesis-dependent LTD stimuli lead to the production of a common set of proteins that are then selected to be used based on the modification of the synapse (Sajikumar and Frey 2004). While the results cannot be directly compared since LTD elicited in vivo with low-frequency stimuli (cross-tagging experiments) is probably mechanistically different from the mGluR-LTD elicited in our studies, our results suggest that specific transport complexes are involved in distinct forms of plasticity. The deficit in L-LTP by Stau1 down-regulation and the impairment of DHPG-induced LTD by Stau2 knockdown strongly support the existence of different mechanisms of regulation for distinct pools of mRNAs and subtype-specific roles for Stau1 and Stau2 in distinct translation-dependent forms of long-term plasticity. Another possibility could be that the partial Stau2 knockdown we observed in slice cultures is sufficient to impair mGluR-LTD but not FSK-induced L-LTP, while a complete knockdown might affect both. Stau2 knockdown animals will be required to test this hypothesis.

Comparison of Stau2 and FMRP knockdown in mGluR-LTD

Another major mRNA-binding protein implicated in mGluR-LTD is FMRP. Comparison of mGluR-LTD studies following Stau2 and FMRP depletion suggests that their roles are more complementary than redundant, since removals of FMRP and Stau2 do not have similar effects. Knockdown of FMRP does not block mGluR-LTD

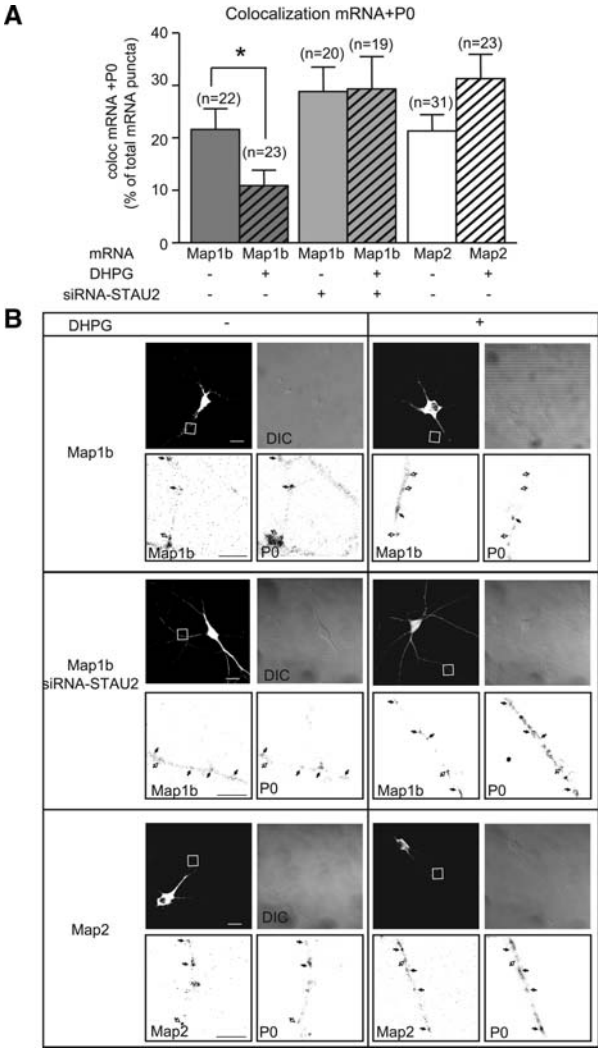

Figure 9. Luc-24xMS2bs-Map1b 3′-UTR mRNA dissociation from P0 upon application of DHPG is prevented by Stau2 siRNA knockdown. (*A*,*B*) Colocalization of NLS-MS2-mCherry-labeled mRNA puncta with P0 in relation to mRNA puncta, with and without DHPG treatment. (*A*) Summary bar graph of colocalization of NLS-MS2-mCherry-labeled mRNA puncta with P0 as percentage of total mRNA puncta (>50 μm from the cell body), showing that DHPG treatment decreases Luc-24xMS2bs-Map1b, but not Luc-24xMS2bs-Map2, mRNA, and P0 colocalization, and the effect is blocked after Stau2 siRNA knockdown. (*B*) Confocal images of representative neurons transfected with Stau2-GFP or siRNA-STAU2-1 with EYFP (*top left* images) and Luc-24xMS2bs-Map1b 3′-UTR or Luc-24xMS2bs-Map2 3′-UTR (*bottom left* images) and immuno-stained for endogenous P0 (*bottom right* images). DIC images are in the *top right*. The boxed area in the *top left* image indicates region shown in *bottom* images. Filled arrows indicate colocalized puncta, and open arrows indicate mRNA puncta alone. n = number of segments from four experiments. $^*P < 0.05$, *t*-test. Error bars represent SEM. Scale bars, 20 μm and 10 μm.

but enhances it and makes it protein synthesis-independent (Hou et al. 2006; Nosyreva and Huber 2006). In contrast, knockdown of Stau2 blocks mGluR-LTD. Removal of Stau2 reduces dendritic levels of an mGluR-LTD-regulated mRNA, while FMRP does not (Bear et al. 2004). While FMRP colocalizes with the Map1b puncta in our study (data not shown), it should be noted that the G quartet thought to be the specific element that associates Map1b with FMRP is in the 5′-UTR of Map1b and is not present in our Map1b 3′-UTR construct. However, this G quartet has not been shown to be required for FMRP regulation of Map1b translation, and FMRP associates with mRNAs using a number of possible motifs.

Dendritic spine defects are not critical for Stau2-dependent mGluR-LTD

As mediators of mRNA transport and translation, some mRNA-binding proteins affect spine morphology, and this deficiency may underlie genetic neurological diseases. Goetze et al. (2006) have shown that Stau2-deficient neurons present a loss of dendritic spines and an increase in filopodia. Our results in young slice cultures also suggest that Stau2 is implicated in synapse formation and spine morphogenesis, although we did not observe a decrease in spine density. This might be due to the use of organotypic slices as opposed to cultured neurons. However, while Stau2 may be important for early development of spines, by the time the neurons have matured, and at the time we are examining translation-dependent mGluR-LTD, the defects are no longer evident. Moreover, in accordance with the intact spine phenotype observed in mature slices after Stau2 knockdown, mEPSCs frequency and amplitude were unchanged, suggesting that basal synaptic function is not affected. Thus the effects of Stau2 knockdown on plasticity are likely due to changes in protein synthesis after induction of mGluR-LTD rather than spine defects.

Stau2 regulates Maplb mRNA distribution during mGluR-LTD

Previous studies showed that Stau1 and Stau2 localize in distinct granules (Duchaine et al. 2002; Thomas et al. 2005) and carry distinct mRNAs (Furic et al. 2008). Consistent with this, we found that siRNA to Stau2, but not to Stau1, specifically lowered the levels of the Map1b 3′-UTR mRNA reporter in dendrites. In contrast, siRNA to Stau1, as previously reported (Kanai et al. 2004), decreased the levels of α-CaMKII 3′-UTR mRNA reporter. Consistently, a recent genome-wide identification of Stau2-bound mRNAs in embryonic rat brains identified Map1b mRNA as a target of Stau2 whereas MAP2 and α-CaMKII mRNAs were absent in Stau2-containing complexes (Maher-Laporte and DesGroseillers 2010).

Stau2 may regulate a specific mRNA granule

Transport of mRNA in dendrites is well established (Carson et al. 2008; Martin and Ephrussi 2009); however, it is unclear whether mRNAs are transported as stalled polysomes in RNA granules or as nascent mRNAs in RNA transport particles (Sossin and DesGroseillers 2006). These two models differ in the mechanism of repression during transport, either at elongation for RNA granules or initiation for RNA transport particles. Indeed, a major controversy in the FMRP field is whether the repression mediated by FMRP is at the level of initiation or elongation (Zalfa et al. 2006). While our data are not definitive, the DHPG-induced dissociation of Map1b 3′-UTR mRNA reporter from P0 staining is consistent with the model that this mRNA was part of an RNA granule. The dissociation would result in a dispersal of the stalled polysomes to near the threshold of antibody detection. For mRNAs in transport particles, we would have expected to see either no change in the colocalization with ribosomes or an increase with the formation of polysomes, depending on the sensitivity of the detection technique. However, at this time, we cannot rule out the alternative explanation that the dissociation of Map1b 3′-UTR mRNA reporter and P0 is due to the completion of translation and reformation of repressed RNA particles not containing ribosomes. The distinction between regulation of RNA granules and transport particles may be important in terms of the time

between granule release and production of full-length protein. mRNAs in stalled polysomes have already been initiated and presumably have produced partial fragments of protein. Once released, the translation process would resume and the rate of synthesis would only depend on elongation factors. In contrast, mRNAs in transport particles have not gone through an initial round of translation and so initiation is the rate-limiting step.

Only a small percentage of the MS2-labeled puncta appear regulated

The use of the MS2 system for following mRNA in cells comes with a few concerns. Despite using an mRNA construct lacking any known localization signals (Luc-24xMS2bs), and looking in dendrites where we would expect minimal contribution from random diffusion, we still saw a comparable number of MS2 puncta (Fig. 7). This may be due to undiscovered localization signals in the luciferase or MS2bs sequences, or to a degree of non-specific binding to transported RNA–protein complexes seen with overexpression. Thus, overexpression of a construct may allow some targeting unseen with endogenous mRNAs. If so, the effect on transport may be underestimated if some of the signal, even 50 μm from the soma, is non-specific. Despite this, we were able to detect significant changes in mRNA localization after disruption of Stau1 or Stau2.

Similarly, to document dissociation of Stau2 from the granule, we examined neurons overexpressing Stau2, although overexpression of RNA-binding proteins may perturb RNA trafficking. Nevertheless, we did observe dissociation of Stau2 from Map1b 3′-UTR mRNA reporter but not from Map2 3′-UTR mRNA reporter under the same conditions, thus demonstrating the specificity of the effect.

Model for Stau 2 function

In the absence of Stau2, we observe both a decrease in the number of Map1b 3′-UTR mRNA reporter puncta in dendrites as well as a decrease in the ability of DHPG to dissociate Map1b 3′-UTR mRNA reporter from P0 staining, suggesting that during mGluR-LTD induction a Stau2-dependent dissociation of Map1b mRNA from P0-containing mRNA granules leads to local protein synthesis resulting in AMPAR internalization and mGluR-LTD (Supplemental Fig. S4). A number of possible explanations are consistent with our data (Supplemental Fig. S4). One possibility is that specific mRNA granules sensitive to DHPG are not formed in the absence of Stau2. The lack of these granules would explain both the reduced transport of Map1b 3′-UTR mRNA reporter in dendrites and the lack of its dissociation. This would also explain the decrease in basal Map1b protein levels in dendrites. Stau2 has been proposed to regulate pre-granule formation in the nucleus and to mediate transport along microtubules (Kiebler et al. 2005; Miki et al. 2005). Thus, interactions of mRNA with Stau2 in the nucleus may recruit additional factors required for the transport and release in the cytoplasm, and the effects of Stau2 knockdown may be in the recruitment of these factors. Second, these granules may be present, but Stau2 would be required specifically for loading Map1b 3′-UTR mRNA reporter into these granules. Finally, Map1b 3′-UTR mRNA reporter may be present in granules, but Stau2 may be specifically required for their translational activation (dissociation of Map1b mRNA and ribosomes from granules). Further characterization of these mRNA–protein complexes and the role of Stau2 will be required to differentiate between these possibilities.

In conclusion, our study demonstrates that Stau1 and Stau2 operate different functions in long-term synaptic plasticity. This specificity is related to their regulation of distinct RNA granules. Our results suggest that Stau2 is implicated in the transport and regulation of Map1b mRNA-containing granules. It will be interesting to characterize further the association of Staufen and mRNA–protein complexes to better understand mechanisms of long-term synaptic plasticity and memory, as well as their role in neurological disorders.

Materials and Methods

Organotypic hippocampal slice cultures

Organotypic hippocampal slices were prepared and maintained in culture as previously described (Stoppini et al. 1991; Lebeau et al. 2008). In brief, Sprague-Dawley rats (postnatal day 7, PN7) were anesthetized and decapitated. The brain was removed and dissected in Hanks' Balanced Salt Solution (HBSS; Invitrogen)–based medium. Cortico-hippocampal slices (400 μm thick) were obtained with a McIlwain tissue chopper (Campden Instruments). Slices were placed on Millicell culture plate inserts (Millipore) and incubated for 3 d in OptiMem (Invitrogen)–based medium at 37°C in a humidified atmosphere of 5% CO_2 and 95% air. Inserts were then transferred to Neurobasal-based medium (Invitrogen). Slices were used for experiments after 4–7 d in culture for young mature slice cultures (PN7 + 4–7 DIV = 11–14 d old) or 14–17 d for older mature slice cultures (PN7 + 14–17 DIV = 21–24 d old).

HEK293 cells

HEK293 cells were grown in Dulbecco's modified Eagle's medium (DMEM) (Invitrogen Life Science), supplemented with 10% Cosmic calf serum (Hyclone), 5 μg/mL penicillin/streptomycin, and 2 mM L-Glutamine (Invitrogen Life Science) and maintained at 37°C saturated with 5% CO_2.

siRNAs and transfections

pEYFP-C1 (EYFP) was obtained from Clontech Laboratories. All siRNAs were purchased from Dharmacon. Commercial siCONTROL was used as non-targeting control siRNA. siRNA target sequences for rat were:

- siRNA-STAU1: 5′-GGACAGCAGUUUAAUGGGAUU-3′ (sense sequence) and 5′-PUCCCAUUAAACUGCUGUCCUU-3′ (antisense sequence) (Lebeau et al. 2008);
- siRNA-STAU2-1: 5′-AGAUAUGAACCAACCUUCAdTdT-3′ (sense sequence) and 5′-PUGAAGGUUGGUUCAUAUCUdTdT-3′ (antisense sequence) (Goetze et al. 2006);
- siRNA-STAU2-2: 5′-CCUACAGAAUGAGCCAAUUUU-3′ (sense sequence) and 5′-PAAUUGGCUCAUUCUGUAGGUU-3′ (antisense sequence) (Goetze et al. 2006).

HEK293 cells were seeded at 2×10^5 in a 6-well plate and transfected with 60 pmol of siRNA-CTL, siRNA-STAU1, siRNA-STAU2-1, or siRNA-STAU2-2 using Lipofectamine 2000 (Invitrogen Life Science). Twenty-four hours post-transfection, cells were transfected again with 100 pmol of the respective siRNA and 1 μg each of plasmids coding for Stau1-HA or Stau-2-HA and hnRNPH1-myc, used as control. Cells were processed for Western blotting 24 h post-transfection. Biolistic transfection of neurons in organotypic slice cultures was performed as previously described (Lebeau et al. 2008), using a Helios gene gun (Bio-Rad) following the manufacturer's instructions. Electrophysiological recordings and cell imaging experiments were performed 48 h after transfection, and the experimenter was blind to transfection treatments.

Electrophysiology

Individual slice cultures were transferred to a submerged-type recording chamber and continuously perfused (at 1–2 mL/min)

with artificial cerebrospinal fluid (ACSF) composed of 124 mM NaCl, 2.5 mM KCl, 1.25 mM NaH_2PO_4, 1.3 mM $MgSO_4$, 26 mM $NaHCO_3$, 10 mM dextrose, and 2.5 mM $CaCl_2$ (5 mM KCl, 2 mM $MgSO_4$, and 2 mM $CaCl_2$ for LTD experiments), saturated with 95% O_2 and 5% CO_2 (pH 7.4). Extracellular field excitatory postsynaptic potentials (fEPSPs) were recorded from CA1 stratum radiatum with a glass microelectrode (2–3 MΩ) filled with 2 M NaCl in slices maintained at 25°C–27°C. Data acquisition (filtered at 2 kHz, digitized at 10 kHz) and analysis were performed using a PC equipped with pClamp9 software (Molecular Devices). A bipolar tungsten electrode placed in stratum radiatum was used for electrical stimulation of Schaffer collaterals. The input–output function was determined at the beginning of each experiment (example in Fig. 2C) to verify optimal placement of electrodes. Note that fEPSPs are typically smaller in amplitude in cultured slices than in acutely prepared slices, because of flattening of the slice in culture conditions. However, with optimal electrode placement, fEPSPs were clearly above detection level and the fEPSP slope was reliably measured (see also Lebeau et al. 2008). Stimulus intensity (0.1 msec duration) was adjusted to elicit 30%–40% of the maximal fEPSP, as determined by an input–output curve for each slice (LTD, 60% of maximal). To reduce spontaneous activity, CA1 and CA3 hippocampal regions were isolated by a surgical cut. The late form of long-term potentiation (L-LTP) was induced chemically by the adenylate cyclase activator forskolin (FSK; 50 μM; Sigma) (Kelleher III et al. 2004; Kopec et al. 2006). Long-term depression (LTD) was induced chemically by the group I metabotropic glutamate receptor (mGluR) agonist (*S*)-3, 5-dihydroxyphenylglycine (DHPG; 100 μM; Ascent). Data analysis of the fEPSP slope was performed on digitized analog recordings using the Clampfit analyze function. Slope measurements (10%–90% of maximal fEPSP amplitude) were obtained with cursors positioned immediately after the stimulation artifact and past the negative peak of the fEPSPs. Typically, 10%–90% slope measurements were taken between 3 and 10 msec poststimulation and thus based on about 70 data points (10 kHz digitization rate). Miniature excitatory postsynaptic currents (mEPSCs) were recorded in whole-cell patch-clamp mode from EYFP-transfected CA1 pyramidal cells using an Axopatch 200B amplifier (Axon Instruments) in slices maintained at 30°C–32°C. Recording pipettes (4–5 MΩ) were filled with a solution containing 130 mM $CsMeSO_3$, 5 mM CsCl, 2 mM $MgCl_2$, 5 mM diNa-phosphocreatine, 10 mM HEPES, 2 mM ATPTris, and 0.4 mM GTPTris (pH 7.2–7.3, 275–285 mOsm). Bicuculline (Bic; 10 μM) and tetrodotoxin (TTX; 0.5 μM) were added to the extracellular solution, and cells were voltage-clamped at −60 mV. Data acquisition (filtered at 2 kHz, digitized at 10 kHz) and analysis were performed using a PC equipped with pClamp9 software (Molecular Devices). Threshold mEPSC amplitude was set at 3 pA, and typically 150–250 events were collected over a 10–20-min period.

Primary hippocampal neurons

Rat primary hippocampal neurons were dissected from embryonic day 17 (E17) to embryonic day 19 (E19) Sprague-Dawley embryos (Charles River Laboratories) and cultured as described (Banker and Goslin 1988; Elvira et al. 2006). Briefly, neurons were plated at 80,000 cells/mL on 18-mm diameter glass coverslips (Fisher Scientific) coated with 0.1% poly-D-lysine. Cells were cultured in Neurobasal medium supplemented with 0.25× GlutaMax, 1% B27 supplement, 1% N2 supplement, and penicillin/streptomycin (GIBCO, Invitrogen). On day 4 and day 11 after plating, half of the media was exchanged for fresh media.

Primary culture transfections

Transfections of 20 pmol of siRNA and 0.3 μg of plasmid coding for EYFP were performed with 2 μL of Lipofectamine 2000 reagent (Invitrogen). For puncta analysis, neurons were transfected on day 13 after plating using Lipofectamine 2000. Briefly, 3 μL of Lipofectamine 2000/50 μL of Neurobasal was combined with 2–3 μg of DNA and/or 20 pmol of siRNA/50 μL of Neurobasal after 5 min. After 20 min, the conditioned media was removed from the cells and saved and the 100 μL of DNA/Lipofectamine mixture was added. The cells were placed for 10 min at 37°C. The transfection media was removed and replaced with conditioned media. DNA used was purified using double-banded CsCl or an endotoxin-free Maxi Prep kit (QIAGEN).

Plasmids

pcDNA-CMV-NLS-HA-MS2-mCherry and pcDNA-CMV-Stau1-Topaz were constructed as previously described (Wickham et al. 1999). pcDNA-SMV-Stau2-GFP was a kind gift from Dr. Michael A. Kiebler (Medical University of Vienna). Luc-24x-MS2 was cloned into pcDNA-RSV. The dendritic targeting element of rat MAP2 3′-UTR was cloned as previously described (Gobert et al. 2008). The full-length mouse CaMKII 3′-UTR (Mayford et al. 1996; Smith and McMahon 2005) was cloned from a previously characterized reporter plasmid (Aakalu et al. 2001), and the full-length rat Map1b 3′-UTR (Accession #NM_019217.1) was cloned from whole rat brain cDNA using the primers 5′-AAAGATATC AAACCGCAGCCGACCACACC-3′ and 5′-TTTCTCGAGGATGTC TCAACACACAAGTGAAC-3′ (underlined are the EcoRV and XhoI restriction sites, respectively, for cloning purpose). These were inserted into the RSV-Luc-24xMS2bs construct to give RSV-Luc-24xMS2bs-Map2 3′-UTR, RSV-Luc-24xMS2bs-CaMKII 3′-UTR, and RSV-Luc-24xMS2bs-Map1b 3′-UTR, respectively.

DHPG treatment and immunocytochemistry

Forty-eight hours post-transfection cultured neurons were treated with 20 μM DHPG (Davidkova and Carroll 2007) (Tocris; Ascent) or vehicle in culture medium for 10 min at 37°C. Immediately after treatment, neurons were rinsed with 1× HBSS (GIBCO), fixed in 4% paraformaldehyde/PBS containing 4% sucrose, and rinsed three times with rinsing buffer (0.5 mM $MgCl_2$, 0.1 M glycine, 1× PBS). Fixed cells were permeabilized (0.1% T × 100, 0.02% NaN_3, 1× PBS) and blocked (5% BSA, 5% goat serum, 0.1% T × 100, 0.02% NaN_3, 1× PBS) at room temperature. The coverslips were placed cell side up on parafilm and incubated in a humid container overnight at 4°C with primary antibody in dilution buffer (0.5% BSA, 5% goat serum, 0.1% T × 100, 0.02% NaN_3, 1× PBS). The cells were washed three times with 1× PBS and incubated in a humid container for 1 h at room temperature with secondary antibody in dilution buffer. The cells were washed three times with 1× PBS and twice with dH_2O prior to mounting on glass slides with Dako fluorescent mounting media (Dako). The primary antibodies used were mouse monoclonal anti-Staufen2 antibodies (Duchaine et al. 2002), human anti-P0 antibodies (ImmunoVision), and anti-Map1b (Santa Cruz). The secondary antibodies used were AlexaFluor 647 goat anti-mouse (dilution 1:200) and goat anti-human IgG (dilution 1:1000) from Molecular Probes (Invitrogen).

Western blotting

Protein samples from hippocampal slices or HEK cell extracts were separated on 10% SDS polyacrylamide gel electrophoresis (PAGE) and transferred onto Amersham Hybond-P (PVDF) membrane. Immunoblots were performed in PBS/0.2% Tween 20 with specific antibodies.

Imaging, morphological, and puncta analysis

For spine analysis, organotypic slice cultures were fixed with 4% paraformaldehyde overnight at 4°C, washed in phosphate buffer, and mounted on slides for confocal microscopy. EYFP-transfected CA1 pyramidal neurons were randomly selected based on green fluorescence and characteristic morphology. Z-stacks consisting of 10–20 sections (512 × 512 pixels, 30–100-μm-long dendritic segments) spaced 0.2–0.4 μm apart were collected from the secondary branches of apical dendrites using confocal laser scanning microscope LSM 510 (Carl Zeiss) equipped with a 63× oil-immersion objective (NA 1.4) (Carl Zeiss). The length and morphology of dendritic spines were analyzed using the LSM 510

software. Three to four independent experiments were performed, and 1505 protrusions were analyzed from 30 neurons. For puncta analysis on dissociated cultured hippocampal neurons, Z-stacks consisting of 10–14 sections (512 × 512 pixels, 30–50-μm-long dendritic segments) spaced 0.4 μm apart were collected from sections of neurites situated at least 50 μm from the cell body. Image J software was used for puncta analysis, and the "analyze particles task" was used to count particles between 0.3 and 1.5 μm in diameter. Colocalization was analyzed and quantified by thresholding the images, and minimal background changes were made for the analysis. For the figures, colors were inverted to ease visualization of the puncta. For colocalization analysis, the coordinates (x, y) of GFP particles were compared to the coordinates of MS2-mCherry and/or anti-P0 particles in the same region; if particle coordinates overlapped, they were considered to be colocalized (Rook et al. 2000). For Map1b immunocytochemistry on dissociated hippocampal neurons, sections of neurites situated from 50 to 100 μm of the cell body were selected for analysis. These regions of interest (ROI) were background subtracted and were analyzed using Image J software. For each condition, 16–18 cells were analyzed from four different experiments.

Acknowledgments

This research was supported by the Canadian Institutes of Health Research (Team Grant to J.-C.L.; CIHR grant MOP 15121 to W.S.S.), Fonds de la recherche en santé du Québec (Groupe de recherche sur le système nerveux central to J.-C.L., W.S.S., L.D.), and the Canada Research Chair Program (Canada Research Chair in Cellular and Molecular Neurophysiology, J.-C.L.). W.S.S. is a James McGill scholar and FRSQ Chercheur National. G.L. was supported by a Savoy Foundation studentship. L.C.M. was supported by a Fonds de la recherche en santé du Québec studentship. We thank Julie Pepin and Catherine Bourgeois for excellent technical assistance.

References

Aakalu G, Smith WB, Nguyen N, Jiang C, Schuman EM. 2001. Dynamic visualization of local protein synthesis in hippocampal neurons. *Neuron* **30:** 489–502.

Andreassi C, Riccio A. 2009. To localize or not to localize: mRNA fate is in 3′UTR ends. *Trends Cell Biol* **19:** 465–474.

Banker G, Goslin K. 1988. Developments in neuronal cell culture. *Nature* **336:** 185–186.

Bear MF, Huber KM, Warren ST. 2004. The mGluR theory of fragile X mental retardation. *Trends Neurosci* **27:** 370–377.

Boda B, Alberi S, Nikonenko I, Node-Langlois R, Jourdain P, Moosmayer M, Parisi-Jourdain L, Muller D. 2004. The mental retardation protein PAK3 contributes to synapse formation and plasticity in hippocampus. *J Neurosci* **24:** 10816–10825.

Bradshaw KD, Emptage NJ, Bliss TV. 2003. A role for dendritic protein synthesis in hippocampal late LTP. *Eur J Neurosci* **18:** 3150–3152.

Bramham CR, Wells DG. 2007. Dendritic mRNA: Transport, translation and function. *Nat Rev Neurosci* **8:** 776–789.

Bramham CR, Worley PF, Moore MJ, Guzowski JF. 2008. The immediate early gene *arc/arg3.1*: Regulation, mechanisms, and function. *J Neurosci* **28:** 11760–11767.

Carson JH, Gao Y, Tatavarty V, Levin MK, Korza G, Francone VP, Kosturko LD, Maggipinto MJ, Barbarese E. 2008. Multiplexed RNA trafficking in oligodendrocytes and neurons. *Biochim Biophys Acta* **1779:** 453–458.

Davidkova G, Carroll RC. 2007. Characterization of the role of microtubule-associated protein 1B in metabotropic glutamate receptor-mediated endocytosis of AMPA receptors in hippocampus. *J Neurosci* **27:** 13273–13278.

Dominguez R, Hu E, Zhou M, Baudry M. 2009. 17β-estradiol-mediated neuroprotection and ERK activation require a pertussis toxin-sensitive mechanism involving GRK2 and β-arrestin-1. *J Neurosci* **29:** 4228–4238.

Duchaine TF, Hemraj I, Furic L, Deitinghoff A, Kiebler MA, DesGroseillers L. 2002. Staufen2 isoforms localize to the somatodendritic domain of neurons and interact with different organelles. *J Cell Sci* **115:** 3285–3295.

Dugre-Brisson S, Elvira G, Boulay K, Chatel-Chaix L, Mouland AJ, DesGroseillers L. 2005. Interaction of Staufen1 with the 5′ end of mRNA facilitates translation of these RNAs. *Nucleic Acids Res* **33:** 4797–4812.

Elvira G, Massie B, DesGroseillers L. 2006. The zinc-finger protein ZFR is critical for Staufen 2 isoform specific nucleocytoplasmic shuttling in neurons. *J Neurochem* **96:** 105–117.

Fitzjohn SM, Kingston AE, Lodge D, Collingridge GL. 1999. DHPG-induced LTD in area CA1 of juvenile rat hippocampus; characterisation and sensitivity to novel mGlu receptor antagonists. *Neuropharmacology* **38:** 1577–1583.

Frey U, Krug M, Reymann KG, Matthies H. 1988. Anisomycin, an inhibitor of protein synthesis, blocks late phases of LTP phenomena in the hippocampal CA1 region in vitro. *Brain Res* **452:** 57–65.

Furic L, Maher-Laporte M, DesGroseillers L. 2008. A genome-wide approach identifies distinct but overlapping subsets of cellular mRNAs associated with Staufen1- and Staufen2-containing ribonucleoprotein complexes. *RNA* **14:** 324–335.

Gobert D, Topolnik L, Azzi M, Huang L, Badeaux F, DesGroseillers L, Sossin WS, Lacaille JC. 2008. Forskolin induction of late-LTP and up-regulation of 5′ TOP mRNAs translation via mTOR, ERK, and PI3K in hippocampal pyramidal cells. *J Neurochem* **106:** 1160–1174.

Goetze B, Tuebing F, Xie Y, Dorostkar MM, Thomas S, Pehl U, Boehm S, Macchi P, Kiebler MA. 2006. The brain-specific double-stranded RNA-binding protein Staufen2 is required for dendritic spine morphogenesis. *J Cell Biol* **172:** 221–231.

Govek EE, Newey SE, Akerman CJ, Cross JR, Van der Veken L, Van Aelst L. 2004. The X-linked mental retardation protein oligophrenin-1 is required for dendritic spine morphogenesis. *Nat Neurosci* **7:** 364–372.

Hengst U, Deglincerti A, Kim HJ, Jeon NL, Jaffrey SR. 2009. Axonal elongation triggered by stimulus-induced local translation of a polarity complex protein. *Nat Cell Biol* **11:** 1024–1030.

Holt CE, Bullock SL. 2009. Subcellular mRNA localization in animal cells and why it matters. *Science* **326:** 1212–1216.

Hou L, Antion MD, Hu D, Spencer CM, Paylor R, Klann E. 2006. Dynamic translational and proteasomal regulation of fragile X mental retardation protein controls mGluR-dependent long-term depression. *Neuron* **51:** 441–454.

Huber KM, Kayser MS, Bear MF. 2000. Role for rapid dendritic protein synthesis in hippocampal mGluR-dependent long-term depression. *Science* **288:** 1254–1257.

Huttelmaier S, Zenklusen D, Lederer M, Dictenberg J, Lorenz M, Meng X, Bassell GJ, Condeelis J, Singer RH. 2005. Spatial regulation of β-actin translation by Src-dependent phosphorylation of ZBP1. *Nature* **438:** 512–515.

Kanai Y, Dohmae N, Hirokawa N. 2004. Kinesin transports RNA: Isolation and characterization of an RNA-transporting granule. *Neuron* **43:** 513–525.

Kelleher RJ III, Govindarajan A, Jung HY, Kang H, Tonegawa S. 2004. Translational control by MAPK signaling in long-term synaptic plasticity and memory. *Cell* **116:** 467–479.

Kiebler MA, DesGroseillers L. 2000. Molecular insights into mRNA transport and local translation in the mammalian nervous system. *Neuron* **25:** 19–28.

Kiebler MA, Jansen RP, Dahm R, Macchi P. 2005. A putative nuclear function for mammalian Staufen. *Trends Biochem Sci* **30:** 228–231.

Kim KC, Kim HK. 2006. Role of Staufen in dendritic mRNA transport and its modulation. *Neurosci Lett* **397:** 48–52.

Klann E, Dever TE. 2004. Biochemical mechanisms for translational regulation in synaptic plasticity. *Nat Rev Neurosci* **5:** 931–942.

Kopec CD, Li B, Wei W, Boehm J, Malinow R. 2006. Glutamate receptor exocytosis and spine enlargement during chemically induced long-term potentiation. *J Neurosci* **26:** 2000–2009.

Krichevsky AM, Kosik KS. 2001. Neuronal RNA granules: A link between RNA localization and stimulation-dependent translation. *Neuron* **32:** 683–696.

Krug M, Lossner B, Ott T. 1984. Anisomycin blocks the late phase of long-term potentiation in the dentate gyrus of freely moving rats. *Brain Res Bull* **13:** 39–42.

Lebeau G, Maher-Laporte M, Topolnik L, Laurent CE, Sossin W, DesGroseillers L, Lacaille JC. 2008. Staufen1 regulation of protein synthesis-dependent long-term potentiation and synaptic function in hippocampal pyramidal cells. *Mol Cell Biol* **28:** 2896–2907.

Lin AC, Holt CE. 2007. Local translation and directional steering in axons. *EMBO J* **26:** 3729–3736.

Maher-Laporte M, DesGroseillers L. 2010. Genome wide identification of Staufen2-bound mRNAs in embryonic rat brains. *BMB Rep* **43:** 344–348.

Martin KC, Ephrussi A. 2009. mRNA localization: Gene expression in the spatial dimension. *Cell* **136:** 719–730.

Mayford M, Baranes D, Podsypanina K, Kandel ER. 1996. The 3′-untranslated region of CaMKII α is a *cis*-acting signal for the localization and translation of mRNA in dendrites. *Proc Natl Acad Sci* **93:** 13250–13255.

McKinney RA. 2005. Physiological roles of spine motility: Development, plasticity and disorders. *Biochem Soc Trans* **33:** 1299–1302.

Miki T, Takano K, Yoneda Y. 2005. The role of mammalian Staufen on mRNA traffic: A view from its nucleocytoplasmic shuttling function. *Cell Struct Funct* **30:** 51–56.
Miniaci MC, Kim JH, Puthanveettil SV, Si K, Zhu H, Kandel ER, Bailey CH. 2008. Sustained CPEB-dependent local protein synthesis is required to stabilize synaptic growth for persistence of long-term facilitation in *Aplysia*. *Neuron* **59:** 1024–1036.
Morita T, Sobue K. 2009. Specification of neuronal polarity regulated by local translation of CRMP2 and Tau via the mTOR–p70S6K pathway. *J Biol Chem* **284:** 27734–27745.
Murphy N, Bonner HP, Ward MW, Murphy BM, Prehn JH, Henshall DC. 2008. Depletion of 14-3-3 zeta elicits endoplasmic reticulum stress and cell death, and increases vulnerability to kainate-induced injury in mouse hippocampal cultures. *J Neurochem* **106:** 978–988.
Nguyen PV, Abel T, Kandel ER. 1994. Requirement of a critical period of transcription for induction of a late phase of LTP. *Science* **265:** 1104–1107.
Nosyreva ED, Huber KM. 2005. Developmental switch in synaptic mechanisms of hippocampal metabotropic glutamate receptor-dependent long-term depression. *J Neurosci* **25:** 2992–3001.
Nosyreva ED, Huber KM. 2006. Metabotropic receptor-dependent long-term depression persists in the absence of protein synthesis in the mouse model of fragile X syndrome. *J Neurophysiol* **95:** 3291–3295.
Otani S, Marshall CJ, Tate WP, Goddard GV, Abraham WC. 1989. Maintenance of long-term potentiation in rat dentate gyrus requires protein synthesis but not messenger RNA synthesis immediately post-tetanization. *Neuroscience* **28:** 519–526.
Otmakhov N, Tao-Cheng JH, Carpenter S, Asrican B, Dosemeci A, Reese TS, Lisman J. 2004. Persistent accumulation of calcium/calmodulin-dependent protein kinase II in dendritic spines after induction of NMDA receptor-dependent chemical long-term potentiation. *J Neurosci* **24:** 9324–9331.
Rook MS, Lu M, Kosik KS. 2000. CaMKIIα 3′ untranslated region-directed mRNA translocation in living neurons: Visualization by GFP linkage. *J Neurosci* **20:** 6385–6393.
Sajikumar S, Frey JU. 2004. Late-associativity, synaptic tagging, and the role of dopamine during LTP and LTD. *Neurobiol Learn Mem* **82:** 12–25.
Sanchez-Carbente MR, DesGroseillers L. 2008. Understanding the importance of mRNA transport in memory. *Prog Brain Res* **169:** 41–58.
Sebeo J, Hsiao K, Bozdagi O, Dumitriu D, Ge Y, Zhou Q, Benson DL. 2009. Requirement for protein synthesis at developing synapses. *J Neurosci* **29:** 9778–9793.
Smith CC, McMahon LL. 2005. Estrogen-induced increase in the magnitude of long-term potentiation occurs only when the ratio of NMDA transmission to AMPA transmission is increased. *J Neurosci* **25:** 7780–7791.
Sossin WS, DesGroseillers L. 2006. Intracellular trafficking of RNA in neurons. *Traffic* **7:** 1581–1589.
Steward O, Schuman EM. 2001. Protein synthesis at synaptic sites on dendrites. *Annu Rev Neurosci* **24:** 299–325.
Stoppini L, Buchs PA, Muller D. 1991. A simple method for organotypic cultures of nervous tissue. *J Neurosci Methods* **37:** 173–182.
Sutton MA, Schuman EM. 2006. Dendritic protein synthesis, synaptic plasticity, and memory. *Cell* **127:** 49–58.
Thomas MG, Martinez Tosar LJ, Loschi M, Pasquini JM, Correale J, Kindler S, Boccaccio GL. 2005. Staufen recruitment into stress granules does not affect early mRNA transport in oligodendrocytes. *Mol Biol Cell* **16:** 405–420.
Waung MW, Pfeiffer BE, Nosyreva ED, Ronesi JA, Huber KM. 2008. Rapid translation of Arc/Arg3.1 selectively mediates mGluR-dependent LTD through persistent increases in AMPAR endocytosis rate. *Neuron* **59:** 84–97.
Wellmann H, Kaltschmidt B, Kaltschmidt C. 1999. Optimized protocol for biolistic transfection of brain slices and dissociated cultured neurons with a hand-held gene gun. *J Neurosci Methods* **92:** 55–64.
Wickham L, Duchaine T, Luo M, Nabi IR, DesGroseillers L. 1999. Mammalian staufen is a double-stranded-RNA- and tubulin-binding protein which localizes to the rough endoplasmic reticulum. *Mol Cell Biol* **19:** 2220–2230.
Zalfa F, Achsel T, Bagni C. 2006. mRNPs, polysomes or granules: FMRP in neuronal protein synthesis. *Curr Opin Neurobiol* **16:** 265–269.

Received December 6, 2010; accepted in revised form February 10, 2011.

Staufen 2 regulates mGluR long-term depression and Map1b mRNA distribution in hippocampal neurons

Geneviève Lebeau, Linda C. Miller, Maylis Tartas, et al.

Learn. Mem. 2011, **18:**
Access the most recent version at doi:10.1101/lm.2100611